Received 14 April 2023; revised 27 June 2023; accepted 1 July 2023. Date of publication 6 July 2023; date of current version 19 December 2023.
The review of this article was arranged by Editor H. Ma.

Digital Object Identifier 10.1109/JEDS.2023.3292824

A High-Precision Circuit-Simulator-Compatible Model for Constant Phase Element Using Rational Function Approximation

YANGKUN HOU [1], TAOMING GUO [1] (Graduate Student Member, IEEE), MANOHAR BANCE [2], AND CHEN JIANG [1] (Member, IEEE)

1 Department of Electronic Engineering, Tsinghua University, Beijing 100084, China
2 Department of Medicine, University of Cambridge, CB2 2QQ Cambridge, U.K.

CORRESPONDING AUTHOR: C. JIANG (e-mail: chenjiang@tsinghua.edu.cn)

This work was supported in part by the National Natural Science Foundation of China under Grant 82151305; in part by the Lingang Laboratory under Grant LG-QS-202202-09; and in part by the National Key Research and Development Program of China under Grant 2019YFA0706100.

This work involved human subjects or animals in its research. Approval of all ethical and experimental procedures and protocols was granted by the University of Cambridge under Application No. HBREC.2018.25.

This article has supplementary downloadable material available at https://doi.org/10.1109/JEDS.2023.3292824, provided by the authors.

ABSTRACT Constant phase elements (CPEs) are commonly used in bioelectronic systems, to model the impedance of bioelectrodes and electrode-electrolyte interfaces. To simulate the systems with an electronic design automation tool, a circuit-simulator-compatible model of the CPE is required to use bioelectrodes in circuit simulation. This paper applies rational function approximation to the impedance of CPEs as a function of frequency, which is able to be implemented with Verilog-A language. In comparison to previously published works which simply approximate a CPE into several serially connected RCs, our work illustrates the theoretical basis behind the approximation with RCs and provides a method perform the approximation, thus resulting in a smaller relative root mean square error of impedance magnitude and phase (4 orders of magnitude lower using 25 RCs) within a bounded frequency range. To validate the model accuracy, it is applied to the modeling of human cochleae, with the simulated results correlating well with the measured results. Furthermore, this model is implemented in a circuit that includes a bioelectrode and a thin-film transistor switch, showing the capability for circuit simulation with CPEs.

INDEX TERMS Constant phase element, verilog-A model, rational function approximation.

I. INTRODUCTION

Bioelectrodes are one of the most important elements in biomedical engineering, by providing the capabilities of electrophysiological measurements, biofuel cells and molecular therapeutic [1], [2], [3]. To predict the electrical performance of a bioelectronic system with bioelectrodes and design a peripheral system for signal control and transmission, the electrical characteristics of bioelectrodes need to be simulated. Thus, equivalent circuit models are constructed. As shown in Fig. 1, the bioelectrode is located in an electrochemical environment. When a current flows through the electrode/electrolyte interface, charge transfer between electrons and ions may take place. The process is rather complicated, which is hard to be modeled by a single resistor or capacitor. Instead, experimentally, the impedances of bioelectrodes fit well by a constant phase element [4], which is an imaginary and mathematical electronic component. The underlying mechanism remains unclear [5], [6]. CPEs are commonly utilized, with high accuracy of behavior modeling both in the time domain and frequency domain [7], [8]. When simulating the electrochemical impedance spectroscopy (EIS) and time domain response of CPEs, the simulation can be performed in several computing platforms (e.g., MATLAB,

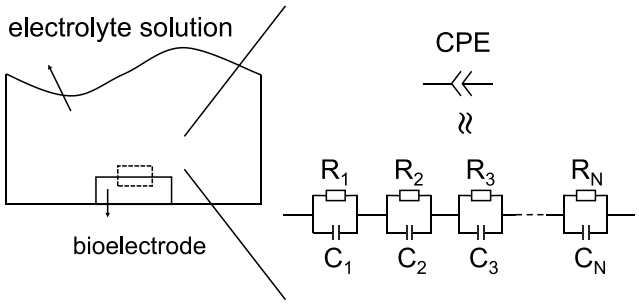

FIGURE 1. Schematic of modeling a bioelectrode as a CPE and approximation of a CPE.

Wolfram Mathematica, etc.) [9], [10]. However, for sensing or stimulating bioelectrodes containing CPEs in a circuit, circuit simulation must be done in simulation program with integrated circuit emphasis (SPICE) simulators [11] (e.g., Cadence, SmartSPICE, etc.) to verify the function of the circuit. Therefore, a circuit-simulator-compatible model for CPEs is necessary.

Though CPEs can be modeled in circuit simulators by both SPICE models and Verilog-A models, Verilog-A models are easier to construct and less costly [12], [13]. SPICE models require not only knowledge of numerical algorithms of the simulators but also good understanding of device physics, while the physical mechanism of CPEs is still not completely clear [5], [6]. Besides, developing a SPICE model takes time and resources due to the complexity of the model. As a result, constructing a SPICE model for CPEs is difficult and costly. In the contrary, Verilog-A is easy to implement due to its high language level. In addition, it is capable of behavioral modeling without any knowledge of device physics [14]. Therefore, it is commonly used in device modeling and suitable for modeling CPEs. Therefore, a Verilog-A model for CPEs is needed for circuit simulation.

There have been time domain and frequency domain modeling techniques for CPEs reported. Most of them use fractional-order transfer function in the frequency domain or fractional differential equations in the time domain to describe the characteristics of CPEs [15], [16]. However, these methods are difficult to implement in Verilog-A, since it is uncappable of dealing with irrational fraction transfer functions or convolution containing irrational fractional calculus in Verilog-A. As shown in Fig. 1, a method that can be implemented in Verilog-A is approximating a CPE with finite and infinite serially connected RC circuits, since resistors and capacitors are fundamental circuit elements [17], [18], [19]. However, these works simply employed RC circuits and focused on optimizing the resistor and capacitor values without figuring out the relationship between using RC circuits and underlying mathematical explanation. Therefore, a Verilog-A model that has clear mathematical explanation behind the approximation is needed.

This paper proposes a Verilog-A model for CPEs after performing rational function approximation to the transfer function of CPE impedance. Our model explains the rationale behind the approximation and leads to improved parameter optimization. Consequently, it has a smaller root mean square (RMS) relative error of impedance magnitude and phase in a bounded frequency range. To verify the model accuracy under different frequency ranges, CPEs with different fractional exponents are modeled in various frequency regions. To verify the accuracy and effectiveness of the model in circuit simulation, the model is incorporated into Cadence for EIS and transient simulation. The results indicate that the model exhibits good accuracy in circuit simulation under a variety of frequency ranges without adding significant computation overhead.

II. CPE ANALYSIS

A. PROBLEMS IN BUILDING VERILOG-A MODEL FOR CPES

CPE is an equivalent electrical circuit component. It is commonly applied in the modeling of electrical components due to its ability to interpret data in the frequency domain with high accuracy and using only two parameters. The phase of a CPE impedance is independent of frequency but related to the fractional exponent α. The impedance of CPE can be expressed by an irrational fraction as:

$$Z_{CPE}(j\omega) = \frac{1}{Q * (j\omega)^{\alpha}} \ (0 < \alpha < 1), \tag{1}$$

where Q represents the magnitude of a CPE impedance at ω=1 rad/s [7]. However, only rational fraction LaPlace transfer functions can be implemented in Verilog-A. Thus, constructing Verilog-A models for CPEs in the frequency domain is difficult.

In the time domain, the relationship between the voltage and current of a CPE is described by

$$v(t) = v(0) + \frac{1}{Q\Gamma(\alpha)} \int_0^t \frac{i(\tau)}{(t-\tau)^{1-\alpha}} d\tau, \tag{2}$$

where $\Gamma(\alpha)$ represents the gamma function [7]. However, convolution is difficult to implement in Verilog-A due to uncertain parameter τ. Hence, a Verilog-A model for CPEs is required.

B. RATIONAL FUNCTION APPROXIMATION OF CPE TRANSFER FUNCTION

Our method performs rational function fitting to the transfer function of CPE impedance, aiming to make it be compatible with Verilog-A. Every rational function can be expressed as the ratio of two polynomials:

$$f(s) = \frac{a_0 s + a_1 s + a_2 s^2 + \cdots + a_N s^N}{b_0 + b_1 s + b_2 s^2 + \cdots + b_M s^M}. \tag{3}$$

The suitable coefficients can be located by rewriting (3) as a linear equation with the form of Ax=b by multiplying both sides with the denominator. However, this problem is badly scaled and conditioned, since the columns in A are multiplied with different powers of s [20]. If the fitting is over a wide frequency range, the approximations will be limited to very low order.

The rational function approximation is an improved equivalent version of a rational function:

$$f(s) = \sum_{n=1}^{N} \frac{c_n}{s - a_n} + d, \tag{4}$$

where residues c_n and poles a_n are either real quantities or complex conjugate pairs, and direct term d is real. The problem is to estimate all coefficients in (4) to reduce the L2 norm error over the given frequency interval. In this work, the rational function approximation of CPEs is performed using the adaptive Antoulas–Anderson (AAA) algorithm [21]. The AAA algorithm is provided in MATLAB for rational function approximation. It is more likely to converge, more accurate and less sensitive to a successful initial value of poles compared with other algorithms (vector fitting, rational Krylov fitting, etc.) [22], [23].

For CPEs, residues are positive real values, poles are negative real numbers, and d is equal to zero. Make the following variable substitutions: $C_n = \frac{1}{c_n}$, $R_n = -\frac{c_n}{a_n}$, (4) is rewritten as:

$$f(s) = \sum_{n=1}^{N} \frac{\frac{1}{C_n}}{s + \frac{1}{C_n R_n}} = \sum_{n=1}^{N} \frac{R_n}{1 + sR_nC_n}, \tag{5}$$

which is the transfer function of N serially connected RCs. As shown in (5), the rational function approximation of the transfer function of a CPE with N poles and residues is equivalent to approximating a CPE into N RCs. As a result, a CPE could be approximated into several serially connected RCs. Note that our model is not a compact model.

As mentioned in the Introduction, there were methods approximating CPEs and other fractional equivalent circuit models into RCs. For example, a ZARC element is a parallel connection of a resistor and a CPE and could be approximated into 3 RCs and infinitely many RCs [19].

As shown in Fig. 2(a), the two methods in [19] and our method with 25 poles provided good fitting for ideal ZARC impedance magnitude under 10 Hz. However, the impedance magnitude provided by the methods in [19] declined rapidly at high frequencies (> 10 Hz), resulting in greater error between the model and ideal ZARC. As shown in Fig. 2(b), the impedance phase provided by the methods in [19] only agreed well with ideal ZARC impedance phase at frequencies below 1 Hz and declined to –90° at high frequencies (> 10 Hz) while the impedance phase provided by our method was in good agreement with ideal ZARC impedance phase from 1 mHz to 1 kHz. The results indicate that rational function approximation provided better fitting for a complex irrational fraction for both magnitude and phase, especially at high frequencies (> 10 Hz). As it is important for bioelectrodes to output stimuli at high frequencies (> 1 kHz), the results also suggest that our method is suitable for circuit simulation with bioelectrodes.

The accuracy of methods in [19] and our method was further evaluated with the RMS relative error, as shown in Fig. 2(c) and (d). Our method shows a high RMS relative error (about 100%) with only 1 pole for both impedance magnitude and phase. As the number of poles increased, the RMS relative error of our method can be significantly controlled, lowered from about 100% using 1 pole to less than 0.001% using 25 poles. This suggests the accuracy of rational function approximation could be improved by using more poles. The methods in [19] had smaller RMS relative

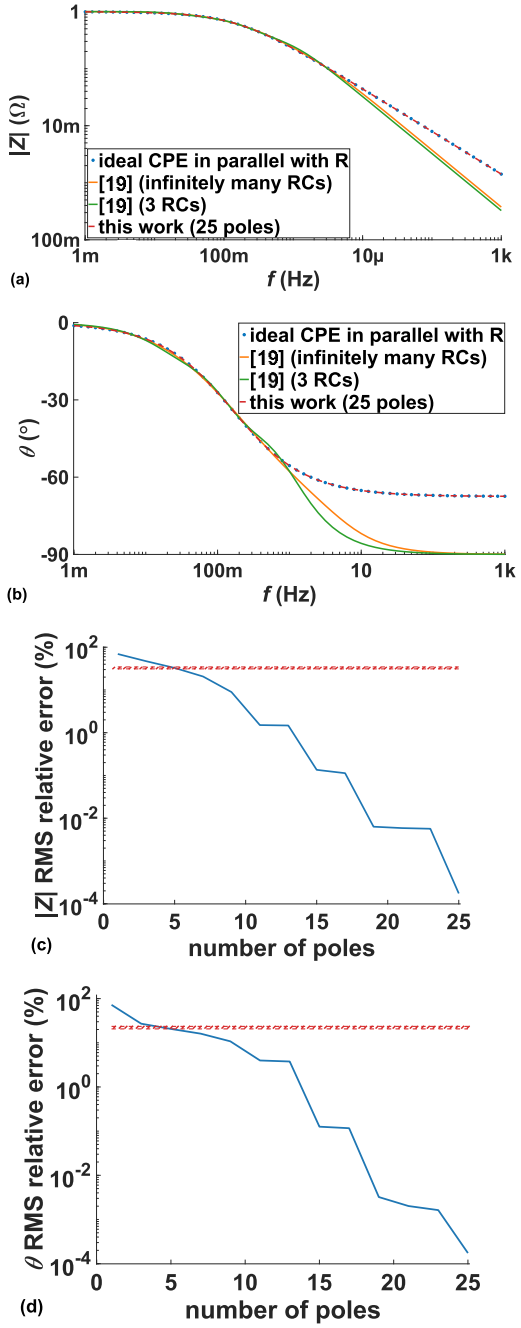

FIGURE 2. [(a) and (b)] The Bode plot of ideal ZARCs with α of 0.75, after RC approximations in [19] and rational function approximation with 25 poles, showing (a) the impedance magnitude and (b) phase. [(c) and (d)] The RMS relative error of ZARCs after RC approximations in [19] and rational function approximation with different poles of (c) the impedance magnitude and (d) phase.

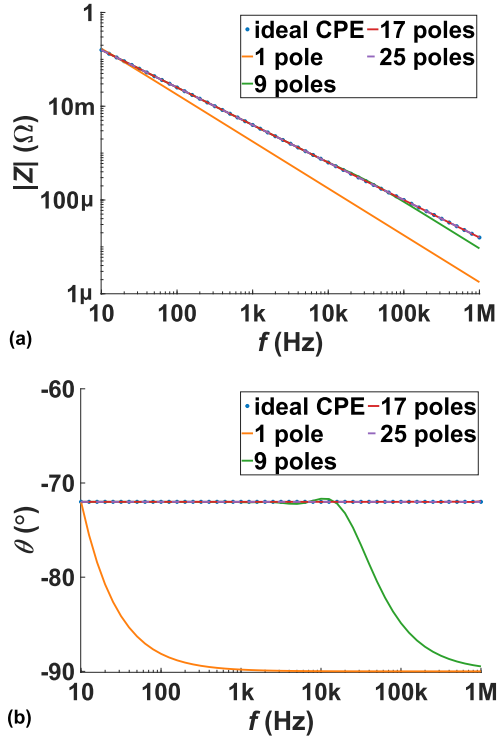

FIGURE 3. [(a) and (b)] The Bode plot of ideal CPEs with α of 0.8 and CPEs after rational function approximation with different poles, showing (a) the impedance magnitude and (b) phase.

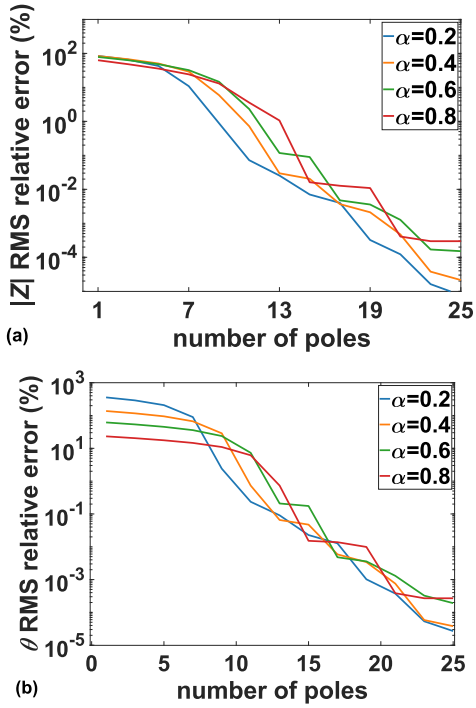

FIGURE 4. [(a) and (b)] The RMS relative error of our models with different α and different poles over the frequency range of (10 Hz,1 MHz) of (a) the impedance magnitude and (b) phase.

error using 3 RCs than our method using 3 poles. However, even by adding infinitely many serially connected RCs, the RMS relative error only decreased 3.5% for impedance magnitude and 2.6% for phase. It suggests that the accuracy of the methods in [19] benefitted little from increasing the number of RCs. As a result, for 7 poles and beyond, our method had smaller RMS relative error for impedance magnitude and phase. The results suggest that the rational function approximation not only revealed the rationale behind the RC approximation, but also contributed to better optimization of values of resistors and capacitors used for the model.

III. RESULTS AND DISCUSSION

A. MODEL ACCURACY

As shown in Fig. 3(a), our model with 1 pole had the same impedance magnitude as the ideal CPE at 10 Hz. As the frequency increased, the gap between our model and ideal CPE became higher. For the model with 9 poles, it provided good fitting for ideal CPE impedance magnitude under 100 kHz with an RMS relative error of 2.2%. However, the error became apparent above 100 kHz and increased with the frequency increasing. For the model with 17 poles and 25 poles, they were in good agreement with ideal CPE from 10 Hz to 1 MHz with the RMS relative error of 1.2% and 0.0003%. As shown in Fig. 3(b), our model with 1 pole had the same impedance phase as the ideal CPE at 10 Hz but started dropping from 10 Hz until it dropped to about $-90°$ at 1 kHz. Our model with 9 poles fitted the ideal CPE impedance phase well from 10 Hz to 10 kHz with the RMS relative error of 0.12% but also dropped to about $-90°$ at high frequencies. The model with 17 and 25 poles performed good fitting for the CPE constant impedance phase from 10 Hz to 1 MHz with the RMS relative error of 0.013% and 0.00027%. The results suggest that for both impedance magnitude and phase, as the number of poles increased, our model fitted ideal CPEs better. In addition, providing good fitting for ideal CPEs required more poles than it at low frequencies. An intuitive explanation was that higher frequencies lead to farther distance between the origin and CPEs in the Nyquist plot, which required more poles and residues for fitting.

The RMS relative error of magnitude and phase of CPE impedance with different α were computed to verify the model universality. As shown in Fig. 4(a), for the impedance magnitude of CPEs with different α, the models had similar RMS relative error of about 100% with 1 pole. As the number of poles increased from 1 to 25, the RMS relative error decreased to less than 0.001%. In addition, the RMS relative error between different models did not show a relationship with α. As shown in Fig. 4(b), the models of CPEs with smaller α had greater RMS relative error of impedance phase with 1 pole. This could result from that as the phase for models with a few poles dropped to –90°, smaller α led to higher phase of ideal CPE impedance and greater RMS relative error. However, as the number of poles increased from 1 to 25, the RMS relative error decreased by four orders of magnitude and also did not show a relationship

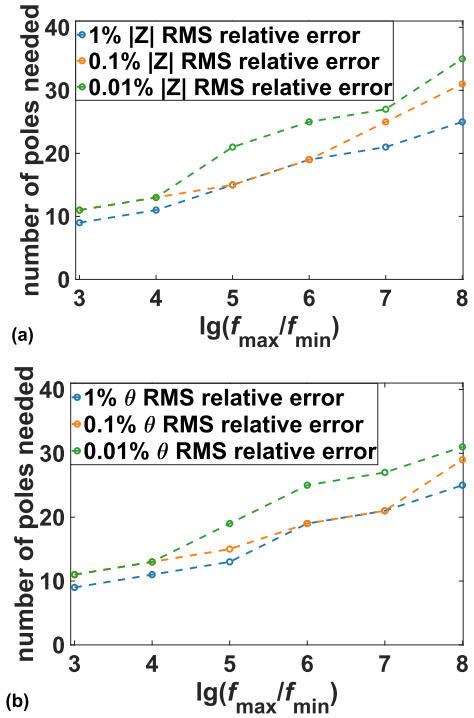

FIGURE 5. [(a) and (b)] Number of poles needed to reach certain RMS relative error of approximating CPEs with α of 0.8, as a function of $\lg(f_{max}/f_{min})$, for the (a) impedance magnitude and (b) phase.

with α. The results suggest that α had an influence on the RMS relative error of impedance phase for models using less than 7 poles, but did not affect the trend that more poles lead to smaller RMS relative error for both amplitudes and phase. The results indicate that rational function approximation was applicable to CPEs with different α. This is because rational function approximation is supposed to be applicable to any irrational function and not affected by the parameters in the irrational function.

We were concerned with various frequency ranges in various scenarios and simulation types. For instance, the frequency range of electrocardiogram bioelectrodes was 0.01 Hz to 1 kHz, whereas the frequency range of electromyogram bioelectrodes was 10 Hz to 100 kHz [24]. In ac simulation, sinusoidal signals mainly drive circuits. Hence, the frequency range of sinusoidal signals was of concern. In transient simulation, pulse signals mainly drive circuits. Therefore, the broad frequency spectrum of pulse signals ranging from relatively low frequencies to the cut-off frequency of the transistor was of concern. In general, it was necessary to study the model accuracy in different frequency ranges.

As shown in Fig. 5(a) and (b), for both impedance magnitude and phase, to lower the RMS relative error under certain level, the model required more poles for wider frequency ranges. For instance, to lower the RMS relative error under 0.01%, as the frequency ranges became wider from 3 decades to 8 decades, the number of poles needed increased from 11 to 35 for magnitude and from 11 to 31 for phase. The results suggest that to offer models with the same accuracy, a broader frequency range would require more complex models. In addition, as the RMS relative error declined, the model required the same or more poles. As more poles resulted in longer simulation time in circuit simulation, the results actually suggest the relationship between the model accuracy and the computation overhead.

It is not necessary to use many poles to our model, though the model with more poles had smaller RMS relative error. The aim of circuit simulation was to predict the performance of bioelectrodes. However, the difference between the results of circuit simulation and the bioelectrode actual behaviors might be affected by various errors, including the error introduced by equivalent circuit models, the error introduced by the CPE Verilog-A models and random error caused by external environment of the bioelectrodes. Only when the error introduced by our models was dominant among all the errors, adding poles in our models would lead to better prediction of the performance of bioelectrodes. In conclusion, the selection of the number of poles depended on not only the RMS relative error of our models, but also errors introduced by other factors.

Figure 5 shows the RMS relative error was a function of $\lg(f_{max}/f_{min})$, where f_{max} represents the maximum frequency of the frequency range and f_{min} represents the minimum frequency of the frequency range. It suggests that the model had the same RMS relative error over different frequency ranges, as long as $\lg(f_{max}/f_{min})$ was the same. The assumption was intuitive that simply shifting the frequency ranges would not have influence on the models. However, the values of poles and residues depended on the concrete implementation of function rational approximation. As a result, RMS relative errors of models over different frequency ranges were compared to verify the assumption.

The models with 3 different frequency ranges had similar RMS relative error (< 0.0001% difference) for CPE impedance magnitude in most instances, as shown in Fig. 6(a). However, when the models had 19 poles or 21 poles, the models had bigger difference in RMS relative error (0.003% using 19 poles and 0.002% using 21 poles). For the impedance phase, as shown in Fig. 6(b), when the models had 19 poles or 21 poles, the difference between models was also bigger (0.007% using 19 poles and 0.006% using 21 poles). The results indicate that the models were not exactly the same when the frequency ranges were different. As the AAA algorithm contained iterations, a change of initial values (frequency ranges) might result in the values of poles and residues. However, the RMS relative error seems to be more dependent on the relative frequency range (i.e., $\lg(f_{max}/f_{min})$) rather than the absolute frequency range.

B. PERFORMANCE IN CADENCE

The modeling and simulation flow of transient simulation is illustrated in Fig. 7. The electrochemical impedance spectroscopy for a bioelectrode is carried out first to perform

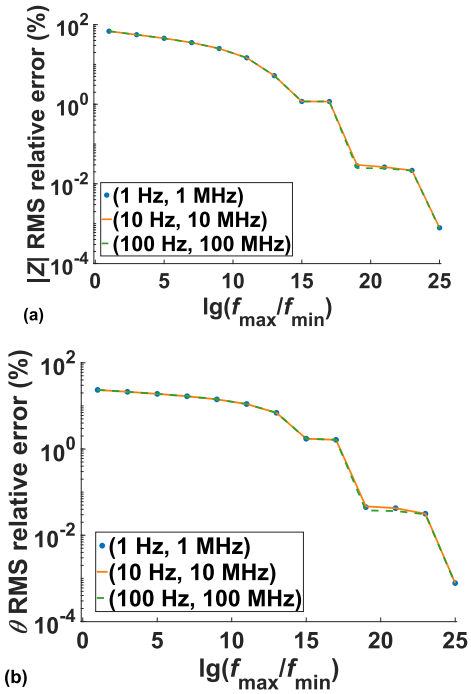

FIGURE 6. [(a) and (b)] The RMS relative error of our models with α of 0.8 and different poles over different frequency ranges, of (a) the impedance magnitude and (b) phase.

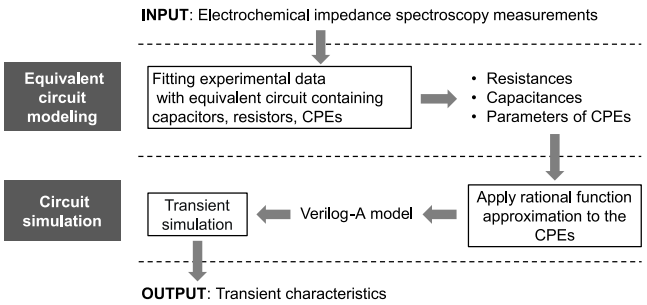

FIGURE 7. Schematic of modeling and simulation flow of transient simulation.

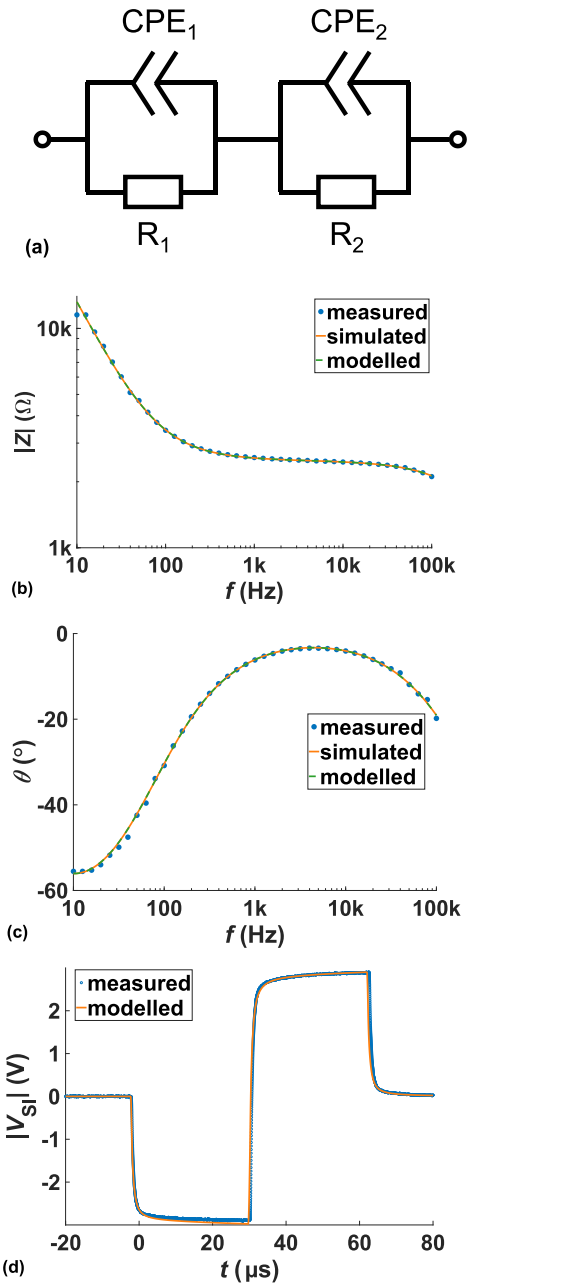

FIGURE 8. (a) Schematic of the equivalent circuit for human cochleae. [(b) and (c)] The Bode plot of human cochleae, showing (b) the impedance magnitude and (c) phase. (d) The simulated and measured spread-induced voltage response as a function of time.

equivalent circuit modeling. The equivalent circuit commonly contains capacitors, resistors and CPEs and the values of these electrical components are extracted by fitting experimental data with equivalent circuit. By applying rational function approximation to the CPEs, the Verilog-A model of the bioelectrode is constructed. After that, the Verilog-A model is incorporated into circuit simulators to perform transient simulation. Finally, the transient characteristics of the bioelectronic circuit and system are obtained.

The accuracy of the model in Cadence was verified by modeling human cochleae. As illustrated in Fig. 8(a), the human cochlea was modeled with two resistor–constant phase element (R-CPE) circuits in series [25]. The measured results from human cadaveric cochleae in full heads were utilized to extract parameters of CPEs and resistors. The simulated results were obtained in MATLAB using ideal CPEs, whereas the modeled results were generated in Cadence using our Verilog-A models with 25 poles. As shown in Fig. 8(b) and (c), both the simulated results and modeled results provided good fitting for the measured results. In addition, the difference between the RMS relative error of the simulated results and modeled results was small for both impedance magnitude (< 0.0004%) and phase (< 0.0005%). The good fitting suggest that the Verilog-A model provided an adequate approximation for CPE impedance in the frequency domain. As shown in Fig. 8(d), the modeled results were in good agreement with measured results

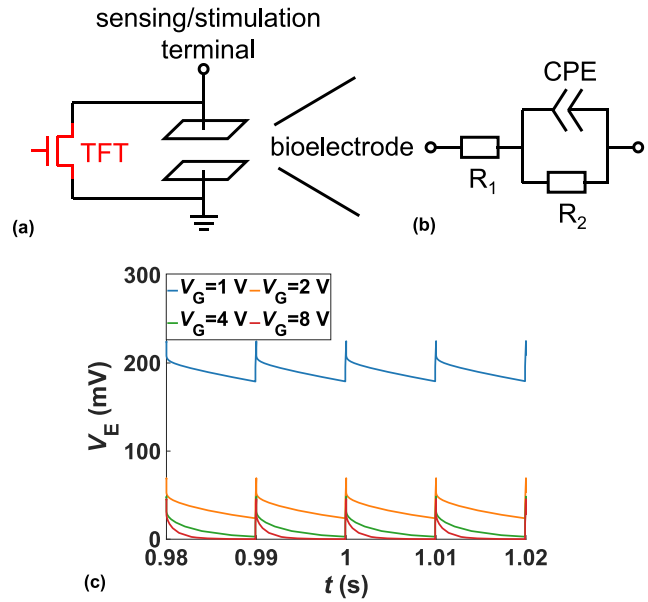

FIGURE 9. (a) Schematic of the 1T circuit for sensing bio-signals or stimulating neurons. (b) Equivalent circuit of the bioelectrode. (c) The simulated voltage of electrodes as a function of time.

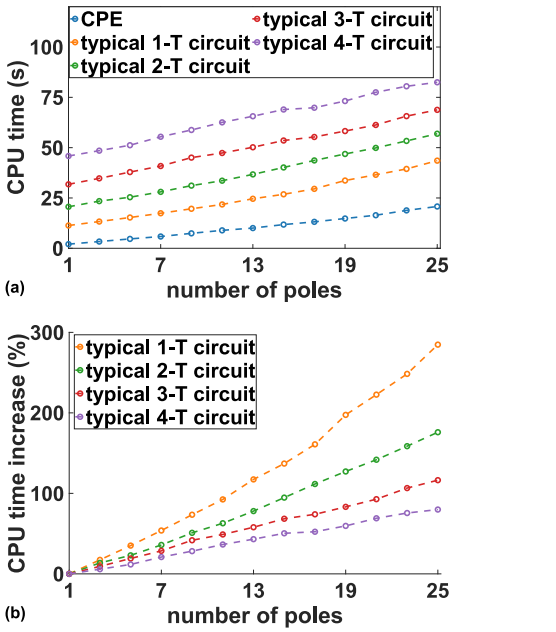

FIGURE 10. (a) Cadence operation time of simulating CPE and circuits as a function of the number of poles of our Verilog-A model. (b) The increase of Cadence operation time as a function of the number of poles of our Verilog-A model in different circuits.

in spread-induced voltage response. This suggests that the model provided good approximation for CPE on stimulation function of bioelectrodes.

A one-transistor (1T) circuit was utilized for stimulating a bioelectrode, as illustrated in Fig. 9(a) [26]. The bioelectrode was modeled as a resistor in series with a parallel circuit of a resistor and a CPE, as shown in Fig. 9(b). The thin-film transistor (TFT) discharged the bioelectrode by operating as a switch. The circuit was driven by two pulse signals with a period of 10 ms. After the electrode was charged for 100 μs, the TFT was switched on for 9900 μs. Our Verilog-A model with 25 poles and a universal compact model [27] were utilized in circuit simulation to validate the circuit functionality. As shown in Fig. 9(c), as the gate voltage of the TFT increases, the voltage of the bioelectrode becomes lower. As the gate voltage of the TFT reaches 8 V, the voltage of the bioelectrode decreases to 0 in every cycle. The results demonstrate that the TFT switch is able to discharge the charges that accumulate between the bioelectrodes. In addition, it demonstrates that our Verilog-A model could be employed for circuit simulation.

Circuit array was commonly used in sensing or stimulation [28]. A pixel circuit usually included several transistors and a bioelectrode containing a CPE. The operation time of a CPE and four typical circuits containing a CPE was obtained in Cadence. Our Verilog-A model with multiple poles and a universal compact model [27] were employed in circuit simulation to record the simulation time. To minimize the influence of Spectre startup time, 1000 duplicates of each circuit were generated in a transient simulation with a stop time of 1μs and a time step of 1ns.

As shown in Fig. 10(a), as the circuit contained more transistors, the operation time went up. In addition, the operation time for simulating a CPE was generally linear to the number of poles. An intuitive explanation was that adding a pole meant adding a RC in the circuit. Furthermore, as the number of poles of our model increased from 1 to 25, the extra time cost for different circuits was similar (< 10% difference). It suggests that the extra time cost brought by our model had no relationship with the circuit complexity. In terms of time complexity, adding a constant amount of time would not change the time complexity of the system. As a result, our model would not change the time complexity of the circuit.

As shown in Fig. 10(b), as the circuit contained more transistors, the increase of operation time introduced by our model decreased. For instance, the model required 15 poles for RMS relative error under 1% for magnitude and phase over the frequency range of (10 Hz, 1 MHz). As the number of poles of our model increased from 1 to 15, the operation time increased by 137.0% in a typical 1T circuit but only 50.4% in a typical 4T circuit. As the circuit becomes more complex, the extra computation overhead introduced by our model is less significant. In conclusion, in a multi-transistor circuit, the extra time cost introduced by our models was insignificant.

IV. CONCLUSION

In conclusion, we proposed a circuit-simulator-compatible model for CPEs with Verilog-A language, allowing simulation of bioelectrodes with CPEs in SPICE-like simulators for biomedical applications. The simulation can support in

both the time domain and the frequency domain. Due to characteristics of CPEs and limitations of Verilog-A, it is difficult to build an ideal CPE model directly in Verilog-A in both the frequency domain and time domain. Thus, the model was implemented after rational function approximation in the frequency domain. The model had small RMS relative error for fitting CPEs with different fractional exponent α. In addition, the model could be utilized in different frequency ranges. The model was used in electrochemical impedance spectroscopy and circuit simulation to validate its precision and effectiveness. The high correlation between the measured and modeled results indicate that our model could be utilized for circuit simulation and exhibited high accuracy. Furthermore, for a circuit with numerous transistors, the additional computational overhead introduced by our model was insignificant. For future work, the methodology of rational function approximation could also be used in sensing function of bioelectrodes, as well as other fractional equivalent circuit models and compact models.

REFERENCES

[1] A. J. Gross, M. Holzinger, and S. Cosnier, "Buckypaper bioelectrodes: Emerging materials for implantable and wearable biofuel cells," *Energy Environ. Sci.*, vol. 11, no. 7, pp. 1670–1687, Jul. 2018, doi: 10.1039/c8ee00330k.

[2] I. Mazurenko, A. de Poulpiquet, and E. Lojou, "Recent developments in high surface area bioelectrodes for enzymatic fuel cells," *Current Opinion Electrochem.*, vol. 5, no. 1, pp. 74–84, Oct. 2017, doi: 10.1016/j.coelec.2017.07.001.

[3] S. Krishnan, "Bioelectrodes for evaluating molecular therapeutic and toxicity properties," *Current Opinion Electrochem.*, vol. 19, pp. 20–26, Feb. 2020, doi: 10.1016/j.coelec.2019.09.004.

[4] S. Mobini, M. U. González, O. Caballero-Calero, E. E. Patrick, M. Martín-González, and J. M. García-Martín, "Effects of nanostructuration on the electrochemical performance of metallic bioelectrodes," *Nanoscale*, vol. 14, no. 8, pp. 3179–3190, Feb. 2022, doi: 10.1039/d1nr06280h.

[5] M. R. S. Abouzari, F. Berkemeier, G. Schmitz, and D. Wilmer, "On the physical interpretation of constant phase elements," *Solid State Ion*, vol. 180, nos. 14–16, pp. 922–927, Jun. 2009, doi: 10.1016/j.ssi.2009.04.002.

[6] A. Lasia, "The origin of the constant phase element," *J. Phys. Chem. Lett.*, vol. 13, no. 2, pp. 580–589, Jan. 2022, doi: 10.1021/acs.jpclett.1c03782.

[7] J. A. López-Villanueva and S. Rodríguez Bolívar, "Constant phase element in thetime domain: The problem of initialization," *Energies*, vol. 15, no. 3, Feb. 2022, doi: 10.3390/en15030792.

[8] M. Grossi and B. Riccò, "Electrical impedance spectroscopy (EIS) for biological analysis and food characterization: A review," *J. Sens. Sensor Syst.*, vol. 6, no. 2, pp. 303–325, Aug. 2017, doi: 10.5194/jsss-6-303-2017.

[9] L. Gagneur, A. L. Driemeyer-Franco, C. Forgez, and G. Friedrich, "Modeling of the diffusion phenomenon in a lithium-ion cell using frequency or time domain identification," *Microelectron. Rel.*, vol. 53, no. 6, pp. 784–796, 2013, doi: 10.1016/j.microrel.2013.03.009.

[10] F. Ciucci, "Modeling electrochemical impedance spectroscopy," *Current Opin. Electrochem.*, vol. 13, pp. 132–139, Feb. 2019, doi: 10.1016/j.coelec.2018.12.003.

[11] A. Vladimirescu, A. R. Newton, and D. O. Pederson, *SPICE Version 2G. 1 user's Guide*. Univ. California Berkeley, Berkeley, CA, USA, 1980.

[12] M. A. Chalkiadaki, C. Valla, F. Poullet, and M. Bucher, "Why- and how- to integrate Verilog-A compact models in SPICE simulators," *Int. J. Circuit Theory Appl.*, vol. 41, no. 11, pp. 1203–1211, Nov. 2013, doi: 10.1002/cta.1833.

[13] C. Jiang, X. Cheng, H. Ma, and A. Nathan, "Flexible electronics and bioelectronics devices," in *Springer Handbook of Semiconductor Devices*. Cham, Switzerland: Springer, 2022, pp. 959–1018.

[14] H. D. L. Verilog, *Verilog-AMS Language Reference Manual*, Accellera Syst. Initiat., Elk Grove, CA, USA, 2014.

[15] S. M. M. Alavi, C. R. Birkl, and D. A. Howey, "Time-domain fitting of battery electrochemical impedance models," *J Power Sour.*, vol. 288, pp. 345–352, 2015, doi: 10.1016/j.jpowsour.2015.04.099.

[16] H. Mu, R. Xiong, H. Zheng, Y. Chang, and Z. Chen, "A novel fractional order model based state-of-charge estimation method for lithium-ion battery," *Appl. Energy*, vol. 207, pp. 384–393, Dec. 2017, doi: 10.1016/j.apenergy.2017.07.003.

[17] E. Kuhn, C. Forgez, P. Lagonotte, and G. Friedrich, "Modelling Ni-mH battery using Cauer and Foster structures," *J Power Sour.*, vol. 158, no. 2, pp. 1490–1497, Aug. 2006, doi: 10.1016/j.jpowsour.2005.10.018.

[18] H. Ren, Y. Zhao, S. Chen, and L. Yang, "A comparative study of lumped equivalent circuit models of a lithium battery for state of charge prediction," *Int. J. Energy Res.*, vol. 43, no. 13, pp. 7306–7315, Oct. 2019, doi: 10.1002/er.4759.

[19] T. Heil and A. Jossen, "Continuous approximation of the ZARC element with passive components," *Meas. Sci. Technol.*, vol. 32, no. 10, Oct. 2021, Art. no. 104011, doi: 10.1088/1361-6501/ac0466.

[20] B. Gustavsen and A. Semlyen, "Rational approximation of frequency domain responses by vector fitting," *IEEE Trans. Power Del.*, vol. 14, no. 3, pp. 1052–1059, Jul. 1999, doi: 10.1109/61.772353.

[21] Y. Nakatsukasa, O. Sète, and L. N. Trefethen, "The AAA algorithm for rational approximation," *SIAM J. Sci. Comput.*, vol. 40, no. 3, pp. A1494–A1522, 2018, doi: 10.1137/16M1106122.

[22] W. Hendrickx and T. Dhaene, "A discussion of "Rational approximation of frequency domain responses by vector fitting"," *IEEE Trans. Power Syst.*, vol. 21, no. 1, pp. 441–443, Feb. 2006, doi: 10.1109/TPWRS.2005.860905.

[23] M. Berljafa and S. Güttel, "The RKFIT algorithm for nonlinear rational approximation," *SIAM J. Sci. Comput.*, vol. 39, no. 5, pp. A2049–A2071, Jan. 2017, doi: 10.1137/15m1025426.

[24] A. H. Umar, M. A. Othman, F. K. C. Harun, and Y. Yusof, "Dielectrics for non-contact ECG bioelectrodes: A review," *IEEE Sensors J.*, vol. 21, no. 17, pp. 18353–18367, Sep. 2021, doi: 10.1109/JSEN.2021.3092233.

[25] C. Jiang, S. R. De Rijk, G. G. Malliaras, and M. L. Bance, "Electrochemical impedance spectroscopy of human cochleas for modeling cochlear implant electrical stimulus spread," *APL Mater.*, vol. 8, no. 9, Sep. 2020, Art. no. 91102, doi: 10.1063/5.0012514.

[26] T. Guo and C. Jiang, "A novel bioelectrode design with an OTFT switch for dynamic discharging," in *Proc. IEEE Int. Flexible Electron. Technol. Conf. (IFETC)*, Qingdao, China, 2022, pp. 1–2, doi: 10.1109/IFETC53656.2022.9948512.

[27] J. Zhao et al., "Universal compact model for thin-film transistors and circuit simulation for low-cost flexible large area electronics," *IEEE Trans Electron Devices*, vol. 64, no. 5, pp. 2030–2037, May 2017, doi: 10.1109/TED.2017.2655110.

[28] F. A. Shaik, S. Ihida, Y. Ikeuchi, A. Tixier-Mita, and H. Toshiyoshi, "TFT sensor array for real-time cellular characterization, stimulation, impedance measurement and optical imaging of in-vitro neural cells," *Biosens. Bioelectron.*, vol. 169, Dec. 2020, Art. no. 112546, doi: 10.1016/j.bios.2020.112546.